Epidermal growth factor receptor downregulation by small heterodimeric binding proteins

Citation: Hackel, B. J., J. R. Neil, F. M. White, and K. D. Wittrup. Epidermal Growth Factor Receptor Downregulation by Small Heterodimeric Binding Proteins. Protein Engineering Design and Selection 25, no. 2 (January 16, 2012): 47-57.

As Published: http://dx.doi.org/10.1093/protein/gzr056

Publisher: Oxford University Press

Persistent URL: http://hdl.handle.net/1721.1/79433

Version: Author's final manuscript: final author's manuscript post peer review, without publisher's formatting or copy editing

Protein Engineering, Design & Selection vol. 25 no. 2 pp. 47–57, 2012
Published online December 9, 2011 doi:10.1093/protein/gzr056

Epidermal growth factor receptor downregulation by small heterodimeric binding proteins

Benjamin J.Hackel[1], Jason R.Neil[2], Forest M.White[2,3] and K.Dane Wittrup[1,2,3,4]

[1]Department of Chemical Engineering, Massachusetts Institute of Technology, Cambridge, MA 02139, USA, [2]Department of Biological Engineering, Massachusetts Institute of Technology, Cambridge, MA 02139, USA and [3]Koch Institute for Integrative Cancer Research, Cambridge, MA 02139, USA

[4]To whom correspondence should be addressed. Department of Chemical Engineering, Massachusetts Institute of Technology, Cambridge, MA 02139, USA. E-mail: wittrup@mit.edu

Received July 11, 2011; revised September 7, 2011; accepted November 10, 2011

Edited by James Marks

No single engineered protein has been shown previously to robustly downregulate epidermal growth factor receptor (EGFR), a validated cancer target. A panel of fibronectin-based domains was engineered to bind with picomolar to nanomolar affinity to multiple epitopes of EGFR. Monovalent and homo- and hetero-bivalent dimers of these domains were tested for EGFR downregulation. Selected orientations of non-competitive heterodimers decrease EGFR levels by up to 80% in multiple cell types, without activating receptor signaling. These heterodimers inhibit autophosphorylation, proliferation and migration, and are synergistic with the monoclonal antibody cetuximab in these activities. These small (25 kDa) heterodimers represent a novel modality for modulating surface receptor levels.

Keywords: downregulation/EGFR/Fn3/heterodimers/yeast display

Introduction

Aberrant signaling from epidermal growth factor receptor (EGFR), a receptor tyrosine kinase in the ErbB family, is implicated in multiple cancers by dysregulation (Yarden and Sliwkowski, 2001), overexpression (Nicholson *et al*., 2001), autocrine signaling (Tateishi *et al*., 1990) and mutation (Pedersen *et al*., 2001; Lee *et al*., 2006; Sharma *et al*., 2007). Ligand-competitive antibodies cetuximab and panitumumab have been approved for clinical use; however, modest efficacy is achieved (Cunningham *et al*., 2004; Bonner *et al*., 2006; Messersmith and Hidalgo, 2007), validating EGFR as a therapeutic target but motivating the development of potentially improved EGFR antagonism.

While predominantly present in a tethered conformation on the cell surface (Burgess *et al*., 2003), binding of growth factor ligands stabilizes an open conformation of EGFR. Resultant dimerization enables kinase activation and phosphorylation of the intracellular domain yielding a complex signaling network that impacts multiple cellular processes including differentiation, migration and growth (Yarden and Sliwkowski, 2001). Potential causes of limited monoclonal antibody efficacy include incomplete ligand competition in the presence of autocrine signaling, insufficient downregulation of receptor and mutational escape. Efficient receptor downregulation would clearly reduce EGFR promotion of tumor formation, proliferation and migration. A previously demonstrated means of receptor downregulation is administration of non-competitive pairs of antibodies (Spangler *et al*., 2010). Antibodies 528 and 806 downregulate EGFR and synergistically inhibit tumor xenografts (Perera *et al*., 2005). Non-competitive antibody pairs 111 + 565 and 143 + 565 downregulate EGFR whereas the competitors 111 + 143 do not (Friedman *et al*., 2005). Also, non-competitive anti-HER2 antibodies downregulate HER2 and inhibit tumor growth (Friedman *et al*., 2005; Ben-Kasus *et al*., 2009). These approaches require dosing two separate agents, compounding regulatory and manufacturing complexity. A single bispecific agent would ameliorate cocktail-related practical issues, as well as enabling construction of multifunctional nano-agents. The tenth type III domain of human fibronectin (Fn3), a 94 amino acid beta-sheet developed for molecular recognition (Koide and Koide, 2007), provides a robust scaffold for bispecific constructs because its single-domain architecture enables simple head-to-tail fusion, which is the natural state of Fn3 domains within the complete fibronectin protein.

In the current work, we use yeast display to engineer a panel of small, single-domain Fn3-based EGFR binders to multiple receptor epitopes. Homo- and hetero-bivalent combinations of these binders, expressed as protein fusions, are tested for the ability to downregulate receptor in a variety of cell lines. Selected non-competitive heterodimers yield up to an 80% reduction in EGFR levels dependent upon epitopes, receptor density and bivalent format. Distinct from ligand-based activation, EGFR downregulation is achieved without substantial receptor agonism. These heterodimers reduce epidermal growth factor (EGF)-induced phosphorylation of extracellular signal-related kinase (ERK) and inhibit proliferation and migration in cells with autocrine signaling.

Materials and methods

Binder engineering

EGFR binders were engineered from the NNB, YS and G4 pooled library as described (Hackel *et al*., 2010). EGFR mutant 404SG (Kim *et al*., 2006) was produced in *Saccharomyces cerevisiae* yeast, purified by metal affinity chromatography and anti-EGFR antibody affinity chromatography, and biotinylated on free amines using the sulfo-NHS

biotinylation kit. The Fn3 yeast surface display libraries were pooled, grown in SD-CAA medium at 30°, 250 rpm and display of Fn3 was induced in SG-CAA medium at 30°, 250 rpm. Binders to streptavidin-coated magnetic Dynabeads were removed. One million biotinylated EGFR ectodomains were loaded on each of 10 million magnetic beads and incubated with the remaining yeast. Beads were washed once with phosphate-buffered saline with bovine serum albumin (PBSA) at 4° and beads with attached cells were grown for further selection. Remaining sorts were conducted with 5 million beads coated with 1–2 million ectodomains. After two sorts, full-length Fn3 clones were selected by fluorescence-activated cell sorting (FACS) using the C-terminal c-myc epitope. Plasmid DNA was zymoprepped from the cells and mutagenized by error-prone PCR of the entire Fn3 gene or the BC, DE and FG loops. Mutants were transformed into yeast by electroporation with homologous recombination and requisite shuffling of the loop mutants. The lead clones and their mutants were pooled for further cycles of selection and mutagenesis. Three rounds, each consisting of two binding sorts on beads, full-length clone isolation by FACS and mutagenesis, were performed. Selection stringency was increased by additional washing and elevated temperature. In the fourth round, a single binding sort on magnetic beads was followed by a binding sort by FACS. Cells were incubated in 10 nM biotinylated ectodomain and mouse anti-c-myc antibody followed by fluorescein-conjugated anti-biotin antibody and R-phycoery thrin-conjugated anti-mouse antibody. Cells with the highest fluorescein:R-phycoerythrin ratio were collected. Three additional rounds of sorting and mutagenesis were performed with decreasing ectodomain concentrations during selections. Plasmids from binding populations were zymoprepped and transformed into *Escherichia coli*; transformants were grown, miniprepped and sequenced.

The relative dominance of E4.2.1 and E4.2.2, as well as very similar mutants, initiated a campaign to identify additional unique clones. Binding populations from rounds two to five were sorted twice for binding to ectodomain in the presence of either ICR10, an antibody that competes with E4.2.2, or 528, an antibody that competes with E4.2.1. Unique clones were identified by sequence analysis.

Fn3 production

The Fn3 gene was digested with NheI and BamHI and transformed to a pET vector containing a HHHHHHKGS GK-encoding C-terminus. The six histidines enable metal affinity purification, and the pentapeptide provides two additional amines for chemical conjugation. The plasmid was transformed into Rosetta (DE3) *E.coli*, which was grown in lysogeny broth (LB) medium with 100 mg/l kanamycin and 34 mg/l chloramphenicol at 37°. Two hundred microliters of overnight culture was added to 100 ml of LB medium, grown to an optical density of 0.2–1.5 units, and induced with 0.5 mM isopropyl beta-D-1-thiogalactopyranoside for 3–24 h. Cells were pelleted, resuspended in lysis buffer (50 mM sodium phosphate, pH 8.0, 0.5 M NaCl, 5% glycerol, 5 mM CHAPS, 25 mM imidazole and 1× complete ethylenediaminetetraacetic acid (EDTA)-free protease inhibitor cocktail), and exposed to four freeze-thaw cycles. The soluble fraction was clarified by centrifugation at 15 000 *g* for 10 min and Fn3 was purified by metal affinity chromatography on TALON resin. Purified Fn3 was buffer exchanged into phosphate-buffered saline (PBS) and biotinylated with NHS-LC-biotin according to the manufacturer's instructions.

An Fn3-linker-Fn3 construct was produced by standard molecular cloning techniques. The resultant vector encodes for Fn3-EIDKPSQ-GSGGGSGGGKGGGGT-Fn3-EIDKPS Q-ELRS-HHHHHH in which the N-terminal Fn3 is bracketed by NheI and BamHI restriction sites and the C-terminal Fn3 is bracketed by KpnI and SacI sites. The reduced linker encodes a GSGT linker. The extended linker is GSGGGSGGGK-GGGSGGGNGGGSGGGGT. Protein was produced as for Fn3.

Affinity titration

A431 or yeast cells were washed in PBSA and incubated with various concentrations of biotinylated Fn3 on ice. The number of cells and sample volumes were selected to ensure excess Fn3 relative to EGFR. For some clones, this criterion necessitates very low cell density, which makes cell collection by centrifugation procedurally difficult. To obviate this difficulty, 'bare' yeast cells are added to the sample to enable effective cell pelleting during centrifugation. Cells were incubated on ice for sufficient time to ensure that the approach to equilibrium was at least 98% complete. Cells were then pelleted, washed with 1 ml PBSA and incubated in PBSA with 10 mg/l streptavidin-R-phycoerythrin for 10–30 min. Cells were washed and resuspended with PBSA and analyzed by flow cytometry. The minimum and maximum fluorescence and the K_d value were determined by minimizing the sum of squared errors assuming a 1:1 binding interaction.

Competition

Yeast displaying EGFR ectodomain or A431 cells were washed and incubated with initial competitor Fn3 or antibody for 30 min. Alternative competitor Fn3, antibody, or AlexaFluor488-conjugated EGF was then added and incubated for 30 min. Cells were washed and secondary reagent was added to detect the alternative competitor: fluorescein-conjugated anti-His antibody, streptavidin-R-phycoerythrin, R-phycoerythrin-conjugated anti-mouse antibody, and fluorescein-conjugated anti-rat antibody for Fn3, biotinylated Fn3, mouse antibodies and rat ICR10, respectively. Cells were washed and analyzed by flow cytometry. Samples with and without initial competitor were compared to determine competition.

EGFR fragment labeling

EGFR ectodomain fragments comprising amino acids 1–176, 294–543 and 302–503 were displayed on the yeast surface (Cochran *et al.*, 2004). Cells were washed and incubated with 30 nM biotinylated Fn3 and mouse anti-c-myc antibody followed by streptavidin-R-phycoerythrin and AlexaFluor488-conjugated anti-mouse antibody. Cells were washed and analyzed by flow cytometry.

Fine epitope mapping

A low mutation library of EGFR ectodomain (Chao *et al.*, 2004) was grown and induced. Yeast was labeled with biotinylated Fn3 and mouse anti-c-myc antibody followed by AlexaFluor647-conjugated streptavidin and AlexaFluor488-

conjugated anti-mouse antibody. Cells were washed and analyzed by flow cytometry. Cells displaying full-length ectodomain (AlexaFluor488^{+}) with reduced Fn3 binding (AlexaFluor647^{weak}) relative to unmutated ectodomain were collected, grown and induced. Cells were then sorted twice for mutants of reduced binding with maintenance of foldedness as determined by binding to antibodies 199.12 or 225, which are conformationally sensitive (Cochran *et al*., 2004). Cells were labeled with biotinylated Fn3 and mouse 199.12 (for clones A, E and E6.2.10) or mouse 225 (for clone D) anti-EGFR antibody followed by AlexaFluor647-conjugated streptavidin and R-phycoerythrin-conjugated anti-mouse antibody. Cells were washed and analyzed by flow cytometry. Cells displaying folded ectodomain (R-phycoerythrin^{+}) with reduced Fn3 binding (AlexaFluor647^{weak}) relative to unmutated ectodomain were collected, grown and induced. Initial selections for clone C mapping yielded multiple glycine mutants and clones with multiple mutations. To improve the efficiency of folded mutants, analogous sorting was performed using the non-competitive domain III binder clone D for foldedness verification. Biotinylated clones C and D were independently complexed to AlexaFluor488- or Alexa Fluor647-conjugated streptavidin and used to label the ectodomain library. Cells that exhibited binding to clone D but reduced clone C binding relative to wild-type ectodomain were collected. Selections for epitope mapping clone B yielded multiple mutants without a consistent location. The full-length ectodomains with reduced clone B binding were sorted for maintenance of clone D binding with a reduction in clone B binding to yield a consistent epitope.

Cell culture

All cells were grown at 37°, 5% CO_2 in a humidified atmosphere. A431 cells were cultured in Dulbecco's modified Eagle medium (DMEM) supplemented with 10% fetal bovine serum (FBS). Chinese hamster ovary (CHO) cells transfected with a vector to express EGFR-green fluorescent protein were cultured in DMEM with 10% FBS, 1% sodium pyruvate, 1% non-essential amino acids and 0.2 g/l G418. HeLa cells were cultured in Eagle's minimal essential medium with 10% FBS. Human mammary epithelial cells (hMEC) cells were cultured in supplemented HuMEC medium. HT29 cells were cultured in McCoy's medium with 10% FBS. U87 cells were cultured in DMEM with 10% FBS, 1% sodium pyruvate and 1% non-essential amino acids. Cells were detached for subculture or assay use with 0.25% trypsin and 1 mM EDTA. For serum starvation, medium was removed by aspiration, cells were washed with warm PBS and fresh serum-free medium was added.

Downregulation assays

Cells were subcultured into 96-well plates, grown for 2 days and serum starved for 12–18 h. Cells were treated with 20 nM Fn3-Fn3 or EGF for the indicated time. Medium was removed by aspiration and cells were washed with PBS, detached with trypsin/EDTA and placed on ice for the remainder of the assay. Bound Fn3-Fn3 or ligand was removed by 5 min acid strip with 0.2 M acetic acid, 0.5 M NaCl. Cells were washed with PBSA and incubated in mouse 225 antibody followed by R-phycoerythrin-conjugated anti-mouse antibody. Cells were washed and analyzed by flow cytometry. Mean fluorescence was normalized to PBSA-treated control samples.

Human embryonic kidney (HEK) transfectants

An EGFR expression vector built on the pCDNA3 vector was used as wild-type or modified by site-directed mutagenesis to introduce T654A, T669A, K721R, Y845F, S1045A/S1046A, Y1068F, Y1148F or Y1173F mutations. Mutations were verified by sequence analysis. HEK cells were grown to 1.2–1.5 million cells per milliliter and diluted to 1 million per milliliter. Miniprepped DNA and polyethyleneimine were independently diluted to 0.05 and 0.1 mg/ml in OptiPro medium and incubated at 22° for 15 min. Equal volumes of DNA and polyethyleneimine were mixed and incubated at 22° for 15 min. 1.2 ml of cells and 48 μl of DNA/polyethyleneimine mixture were added to a 24-well plate and incubated at 37°, 5% CO_2 with shaking for 24 h. One hundred microliter aliquots of each transfection were transferred to a 96-well plate and grown for 24 h. A downregulation assay was performed as described.

In-cell western blot

A431 cells were cultured in 96-well plates, serum starved for 12–24 h and treated with 20 nM Fn3-Fn3 or EGF. Cells were fixed for 10 min by addition of an equal volume of 4% formaldehyde. Cells were washed and permeabilized with four washes of PBS with 0.1% Triton X100 and blocked in Odyssey blocking buffer for 2 h at 22° or overnight at 4°. Cells were incubated in 10 nM rabbit anti-phospho(S/T/Y) for 2 h at 22° or overnight at 4°. Four washes in PBS with 0.1% Tween20 were followed by 33 nM 800CW-conjugated anti-rabbit antibody and 180 nM ToPro3 and four additional washes. Plates were imaged at 700 and 800 nm. Antibody signal (800 nm) was normalized to DNA (700 nm) for each well.

Western blot

A431 cells were cultured in 24-well plates and serum starved for 16 h. For agonism assay, cells were treated with 20 nM Fn3-Fn3, antibody or EGF for 15 min. For antagonism assay, cells were treated with Fn3, Fn3-Fn3 or antibody for 6 h followed by 1 nM EGF for 15 min. Medium was removed by aspiration and cells were washed twice with cold PBS and lysed for 5 min in 50 μl of RIPA buffer with protease and phosphatase inhibitors and EDTA (Pierce). Lysates were clarified by centrifugation at 14 000 *g* for 15 min, separated by sodium dodecyl sulfate polyacrylamide gel electrophoresis (SDS–PAGE) on a 12% BisTris gel, and blotted to nitrocellulose. Blots were blocked in 5% non-fat dry milk and labeled with 1:1000 anti-phosphoERK1/2 Y202/Y204 antibody (Cell Signaling, Danvers, MA) followed by peroxidase-conjugated anti-rabbit antibody. Blots were incubated in SuperSignal West Dura substrate and imaged. Blots were then washed extensively, labeled with rabbit anti-GAPDH antibody followed by peroxidase-conjugated anti-rabbit antibody, incubated with substrate and imaged. PhosphoERK1/2 Y202/Y204 labeling was normalized by GAPDH signal.

Quantitative phosphoproteomics

A431 cells were cultured in 12-well plates, serum starved for 16 h and treated with 20 nM Fn3-Fn3, Fn3 + Fn3 or EGF for 15 or 60 min. Medium was removed by aspiration and cells were washed with PBS and lysed in 8 M urea with 1 mM Na_3VO_4. Lysates are digested to form peptides and labeled with iTRAQ reagents. Phosphotyrosine-containing peptides

are isolated by immunoprecipitation with a pool of polyclonal anti-phosphotyrosine antibodies and phosphopeptides are enriched by immobilized metal affinity chromatography. Peptides are separated and analyzed by liquid chromatography–mass spectrometry (LC–MS)/MS. Peptides are identified using MASCOT and relative abundance is determined by comparison of peak intensities.

Proliferation

hMEC cells transfected with a vector for membrane-bound EGF ligand with a transforming growth factor α (TGFα) cytoplasmic tail (hMEC + TCT (Joslin *et al*., 2007)) were obtained from Doug Lauffenburger (MIT). Eight thousand cells were plated into each well of a 96-well plate and incubated in 100 μl of medium with 20 nM agent for 48 or 96 h. For 96 h samples, medium was supplemented with fresh agent at 48 h. Cell viability was quantified using the AlamarBlue assay (Invitrogen) according the manufacturer's instructions and normalized to PBSA-treated control.

Migration

hMEC, hMEC cells transfected with a vector for membrane-bound EGF ligand (hMEC + ECT) or hMEC + TCT cells were cultured in 96-well plates to confluent monolayers. Wounds were scratched into the monolayer using a pipette tip, and cells were washed with fresh medium and imaged on a Nikon confocal microscope with robotic stage. Cells were treated with 20 nM agent in 100 μl of medium, incubated for 24 or 48 h, and imaged at identical fields of view. Migration was quantified as the average reduction in separation across the wound and normalized to PBSA-treated control.

Results

Fn3-based binder engineering

Multiple high-affinity binders to distinct epitopes of EGFR ectodomain were isolated by yeast display of a fibronectin-based scaffold library. As previously described, a yeast surface display library (Hackel *et al*., 2010) of Fn3 clones was sorted for binding to biotinylated soluble EGFR ectodomain (Kim *et al*., 2006) using magnetic bead selections (Ackerman *et al*., 2009) and flow cytometry. Directed evolution was performed on a population of lead clones using recursive dual mutagenesis with loop shuffling as described (Hackel *et al*., 2008). Two clones dominated the sequenced population after five rounds of evolution. Competition against existing anti-EGFR antibodies revealed that clone E4.2.1 is competitive with 528, a domain III binder (Cochran *et al*., 2004), and clone E4.2.2 is competitive with ICR10, a domain I binder (Cochran *et al*., 2004). To identify additional binders, intermediate populations were sorted for binding to EGFR ectodomain in the presence of 528 or ICR10. Five unique clones that bound ICR10-blocked EGFR were identified: EI4.4.2, EI3.4.3, EI3.4.2, EI2.4.6 and EI1.4.1. Also, two additional rounds of sorting with unblocked EGFR yielded an improved mutant of E4.2.2 named E6.2.6 and one additional clone, E6.2.10. Clones were renamed A–H for simplicity (Table I). The affinity of each clone was determined by titration of biotinylated Fn3 binding to A431 cells (on ice to prevent internalization); affinities ranged from 250 pM to 30 nM (Table I).

Table I. EGFR-binding Fn3 domain sequences and affinities

		Sequence				K_d (nM)			Epitope			
Name	Alias	BC loop	DE loop	FG loop	Framework	A431, pH 7.4	A431, pH 5	Yeast, pH 7.4	EGFR mutants	Domain	Ab. Comp.	Fn. Comp.
Wild type	WT	DAPAVTVRY	GSKST	GRGDSPASSK	–	nb	nb	nb	–	–	–	–
E6.2.6	A	FDYAVTY	GWIST	DNSHWPFRST	I90T	0.26 ± 0.13	0.26 ± 0.14	1.2 ± 0.4	L14H, Q16R, Y45F, H69(Q,R,Y)	D1	ICR10	None
E4.2.1	B	YGFSLASS	RSPWF	SNDFSNRYSG	–	30 ± 3	2.5 ± 0.7	0.25 ± 0.07	I327K, V350M, F352V, W386R	D3	225	C,E
EI4.4.2	C	YFRDPRYVDY	WYLPE	GDDQNAGL	V45A	1.4 ± 0.2	0.64 ± 0.32	4 ± 4	I341V, E376K	D3	225	B,E
EI3.4.3	D	LHHRSDVRS	GSRSL	WGSYCCSN	E47K	0.25 ± 0.05	0.081 ± 0.044	2.5 ± 0.1	K430E, S506R	D3/D4	Neither	None
EI2.4.6	E	YHPFYYVAHS	RSPWF	DSNGSH	–	2.9 ± 0.3	nb	4 ± 4	T235M, F335I, V350M, A351T, F352L, T358A	D3	225	B,C
E6.2.10	F	YLRDPRYVDY	WYLPE	YDGYRESTPL	–	0.96 ± 0.11	0.88 ± 0.64	–	K311N, I332T	D3	–	–
EI3.4.2	G	YGSSYASY	RSPWF	PSGISA	T58I	9.5 ± 3.5	0.80 ± 0.28	1.0 ± 0.2	–	–	–	–
EI1.4.1	H	YGPFYYVAHS	RSPWF	SKCYDGSV	–	0.85 ± 0.50	–	0.06 ± 0.04	–	–	–	–

K_d indicates equilibrium dissociation constant for binding to A431 cells on ice or yeast at 22°. nb indicates no detectable binding. – indicates data not collected. EGFR mutants indicate ectodomain mutants that demonstrate reduced affinity for the indicated clone. Domain indicates the EGFR domain(s) in which the epitope resides. Ab. Comp. indicates whether ICR10 or 225 are competitive with the indicated clone. Fn. Comp. indicates whether clones A, B, C, D or E are competitive with the indicated clone.

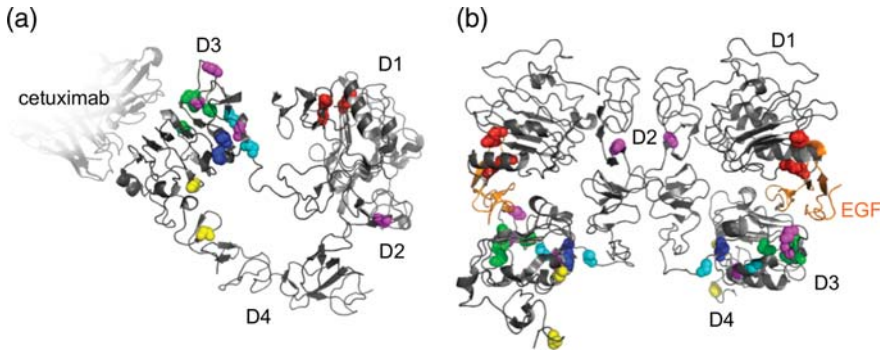

Fig. 1. Epitope mapping of EGFR-binding Fn3 domains. A library of EGFR ectodomain mutants was sorted for clones that maintained binding to a conformational binder but had reduced binding to the indicated Fn3 domain. All single amino acid mutants, excluding proline and glycine mutants, are presented as spheres in the crystal structures of (**a**) the tethered monomer (1NQL; Ferguson *et al*., 2003) and (**b**) the ligand-bound dimer (1IVO; Ogiso *et al*., 2002). Mutations: clone A (red): L14H, Q16R, Y45F and H69(Q,R,Y); clone B (green): I327K, V350M, F352V and W386R; clone C (blue): I341V and E376K; clone D (yellow): K430E and S506R; clone E (magenta): T235M, F335I, V350M, A351T, F352L and T358A; clone F (cyan): K311N and I332T. Cetuximab is shown in (a) based on homology to the crystal structure of the EGFR/cetuximab complex (1YY9; Li *et al*., 2005). EGF is shown in orange in (b). Domains are labeled D1–D4.

Competition and epitope mapping

Fine epitope mapping was performed for clones A–F by high throughput identification of EGFR mutations that maintain other conformational epitopes but have reduced affinity for the clone of interest (Chao *et al*., 2004). Clones G and H were excluded because of sequence similarity and binding competition with clones B and E, respectively. Clones B, C, E and F all bind the N-terminal half of domain III (Fig. 1), which is consistent with complementary Fn3 competition as well as EGF competition (data not shown). Clones B, C and E also compete with antibody 225 for binding, which is reasonable given their proximity to the cetuximab (a 225 chimera) interface (Fig. 1a). The absence of competition between clone F and 225 is consistent with their distinct, though adjacent, epitopes. The clone A epitope resides in domain I, as expected given its observed competition with EGF and ICR10 antibody, and the ability of clone A to label EGFR ectodomain fragment comprising amino acids 1–176 as well as the lack of competition with the other Fn3 domains (data not shown). Clone D binds a novel epitope near the interface of domains III and IV, which is consistent with its ability to label fragments 294–543 and 302–503 as well as its lack of competition with antibodies 225 and ICR10 and the other Fn3 domains (data not shown). Clone D competes with EGF, which cannot readily be attributed to direct steric inhibition given their distal binding epitopes. However, a reasonable hypothesis is that clone D binding interferes with receptor untethering that supports high-affinity ligand binding. Although domains III and IV do not grossly change during untethering (Burgess *et al*., 2003), subtle rearrangements at the domain III/domain IV interface exist; for example, amino acids 430 and 506, which are the sites identified in clone D epitope mapping, move from 19.7 Å apart in the tethered structure to 16.7 Å in the dimer. Thus, at least three classes of binders were engineered and mapped: clone A binds to domain I; clones B, C and E bind domain III and are competitive with each other and antibodies 225 and 528; and clone D binds to the C-terminal portion of domain III and the N-terminal portion of domain IV and does not compete with antibodies 225 and 528 nor clones B, C and E.

Downregulation by heterobivalent constructs

Given the previously reported success of particular pairs of non-competitive homobivalent antibodies to downregulate EGFR, we were interested to determine whether downregulation could be accomplished with a single heterobivalent agent. Fn3 clones were linked as head-to-tail protein fusions with the native peptide linker EIDKSPQ as well as a flexible GSGGGSGGGKGGGGT linker (Fig. 2a). Thirty constructs comprising all possible bivalent combinations, in both orientations, as well as monomer for clones A–E (heterodimers are named N–C where N and C represent the N-terminal and C-terminal Fn3 clones) were tested. Three different EGFR-expressing human cell lines were tested: A431 epidermoid carcinoma, HeLa cervical carcinoma and HT29 colorectal carcinoma. Cells were cultured, serum starved and incubated with 20 nM Fn3 or Fn3-Fn3 for 6–8 h. Cells were detached, bound agent was acid stripped and surface EGFR was quantified by flow cytometry. Although many constructs did not modify surface EGFR levels relative to control, heterodimers D-B, D-C, D-D, D-E, A-D, B-D, C-D and E-D downregulate, yielding up to 80% reduction in surface EGFR; D-B, D-C and D-E have the greatest effect (Fig. 2b and c). Particular combinations of non-competitive clones in a heterobivalent construct are needed to downregulate although the D-D homobivalent does moderately reduce receptor levels. The particular success of heterodimers incorporating the D domain is noteworthy. Curiously, particular orientations of combinations are needed; for example A-D downregulates whereas D-A does not.

To examine the impact of EGFR expression level, three heterodimers were tested on additional cell lines: U87 glioblastoma, hMEC and CHO cells transfected with EGFR-green fluorescent protein fusion. Downregulation was observed in all six cell lines for D-B, D-C and D-E (Fig. 3a). Interestingly, downregulation was lesser for D-C and D-E in the low-expressing cells HT29 and U87. Conversely, EGF downregulates receptor most robustly in these low-expressing lines while exhibiting muted receptor reduction in the high-expressing CHO and A431 cells. Downregulation kinetics were analyzed for the most robust heterodimers. D-B and D-C downregulate EGFR in A431 cells with half-times of 1.1 and

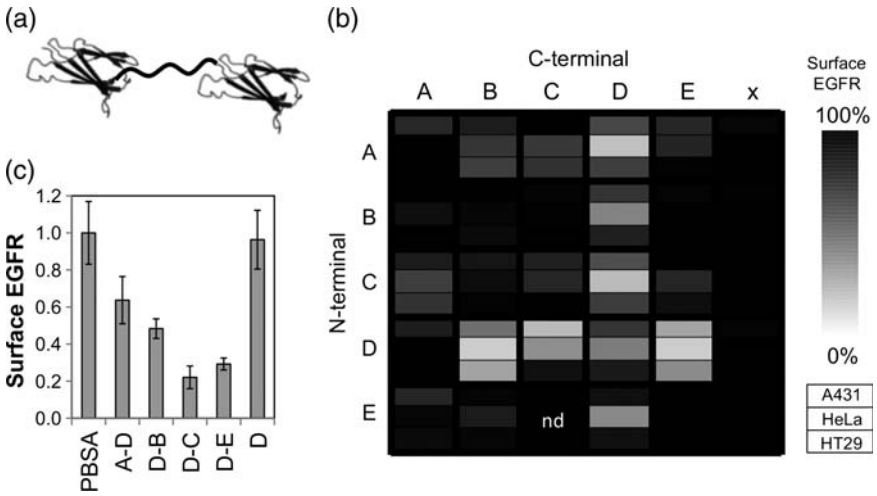

Fig. 2. EGFR downregulation. (**a**) Schematic of Fn3-Fn3 heterobivalent with the wild-type Fn3 structure from PDB ID 1TTG and the flexible linker drawn approximately to scale in cartoon form. (**b**) A431, HeLa and HT29 cells were cultured in 96-well plates, serum starved and treated with 20 nM of the indicated Fn3 or Fn3-Fn3 construct for 6–8 h. Surface EGFR was quantified by flow cytometry and is presented on a color scale relative to PBSA-treated control with black indicating no downregulation and white indicating complete downregulation. Mean of triplicate samples is used for quantification. (**c**) Data from (b) for select constructs with A431 cells. Error bars indicate standard deviation of triplicate samples. PBSA indicates PBS with bovine serum albumin.

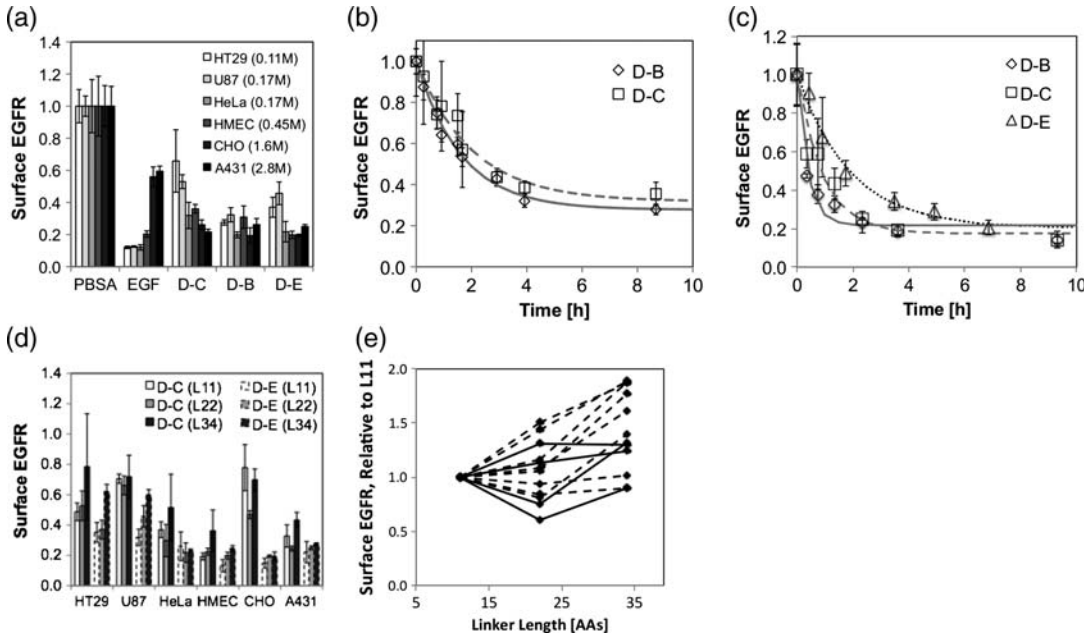

Fig. 3. Downregulation characterization. Cells were cultured in 96-well plates, serum starved and treated with 20 nM agent for 8 h unless noted. Surface EGFR was quantified by flow cytometry and normalized to PBSA-treated control. Values and error bars indicate the mean and standard deviation of triplicate samples. (**a**) Cell line and receptor density impact. Downregulation was quantified in six cell lines of varying EGFR levels. Parenthetical notation in legend indicates the number of EGFR per cell in million. (**b, c**) Downregulation kinetics. Downregulation was quantified at multiple time points in A431 (b) and HeLa (c) cells. Lines represent a theoretical fit of the data calculated by minimizing the sum of squared errors. (**d**) Linker length impact. The downregulation assay was performed with D-C (solid outline) and D-E (dashed outline) heterodimers with linkers of 11, 22 or 34 amino acids. (**e**) The data from (d) are summarized to compare linker lengths. Surface EGFR values are normalized for each combination and cell type. Dashed lines indicate cells with <1 million EGFR per cell. Solid lines indicate cells with >1 million EGFR per cell.

1.4 h, respectively (Fig. 3b). Downregulation in HeLa cells is slightly faster at 0.44, 0.59 and 1.3 h for D-B, D-C and D-E (Fig. 3c).

Heterobivalent D-C and D-E constructs were created with three different lengths of the linker between the Fn3 domains; in addition to the native EIDKPSQ glycine-rich linkers of 4, 15 or 27 amino acids were included. These constructs were tested for downregulation of EGFR in HT29, U87, HeLa, hMEC, CHO and A431 cells (Fig. 3d). There is a general trend towards less effective downregulation with longer linker length (Fig. 3e), although the effect varies among the cell lines (Pearson correlation coefficients of 0.64 and 0.36 for cells with less than or greater than, respectively, 1 million EGFR).

An alternative format of bispecific oligomers was tested in which monovalent Fn3 domains were biotinylated and

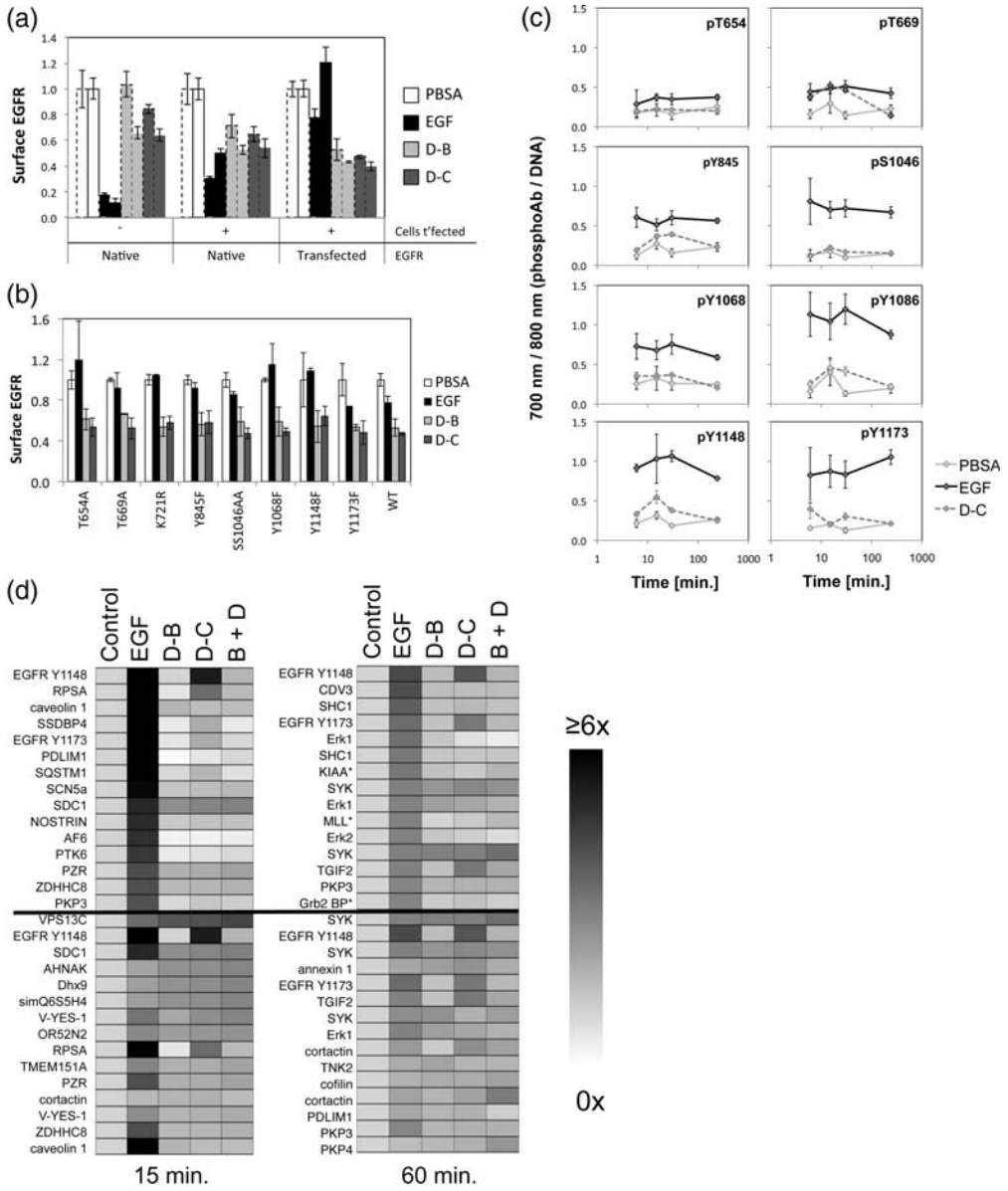

Fig. 4. Intracellular effects of downregulation. (**a**) Downregulation of EGFR in HEK transfectants. HEK cells were transfected with an EGFR expression vector, grown and treated with 20 nM agent for 2 h (dashed outline) or 7 h (solid outline). Surface EGFR was quantified by flow cytometry and normalized to PBSA-treated control. Three conditions are shown: untransfected cells; untransfected cells in the presence of transfected cells, and transfected cells. (**b**) Downregulation of mutant EGFR. HEK cells were transfected with the indicated EGFR expression vector, grown and treated with 20 nM agent for 2 h. Surface EGFR was quantified by flow cytometry and normalized to PBSA-treated control. (**c**) EGFR phosphorylation. A431 cells were cultured in 96-well plates, serum-starved and treated with 20 nM agent for 5, 15, 60 or 240 min. Cells were fixed, permeabilized, labeled with rabbit anti-phosho-(S/T/Y) antibody followed by anti-rabbit-800CW and ToPro3 (to stain DNA) and imaged. (**d**) Proteomic phosphorylation. A431 cells were cultured in 12-well plates, serum starved and treated with 20 nM agent for 15 or 60 min. Cell lysates were reduced, alkylated, digested and labeled with iTRAQ isotopic labels. Peptides with phosphorylated tyrosines are isolated by polyclonal antibody affinity chromatography and analyzed by LC–MS/MS. Relative phosphorylation is quantified by comparison of isotopically related peaks. Top portion represents 15 highest responders to EGF treatment. Lower portion represents 15 highest responders to heterobivalent treatment.

combinations of clones were immobilized on AlexaFluor488-conjugated streptavidin. In all bispecific and trispecific combinations of A, C, D, E, G and H, no downregulation is observed in HT29 or U87 cells transfected to overexpress EGFR (data not shown). Yet most combinations yield a substantial accumulation of internalized AlexaFluor488 signal, consistent with internalization without downregulation. Thus, the particular oligomeric topology appears critical for efficacy. Of note, internalized AlexaFluor488 signal at 37° correlates with surface labeling at 4° (which restricts internalization) suggestive of passive internalization for all combinations of streptavidin-based oligomers. The ineffectiveness of this oligomeric topology further highlights the existence of stereospecific requirements for the presumptive crosslinking-mediated downregulation.

Absence of significant agonism by fibronectin heterodimers

To investigate the mechanisms of downregulation, an EGFR expression vector was transfected into HEK cells, which themselves constitutively express low levels of native EGFR. Although EGF robustly downregulates native HEK EGFR, transfected cells with ~50-fold more EGFR are not

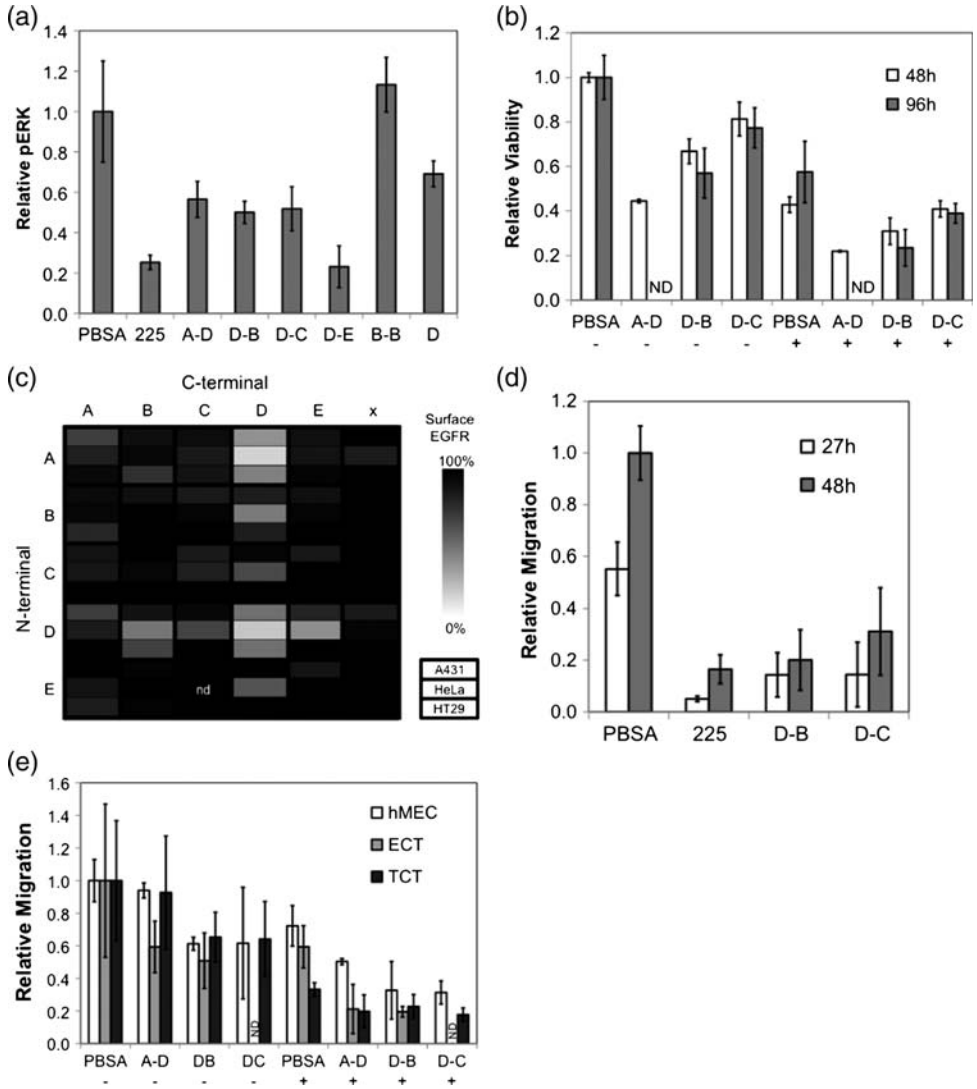

Fig. 5. Downstream effects of EGFR downregulation. (**a**) Inhibition of ERK phosphorylation. A431 cells were cultured in 24-well plates, serum starved and treated with 20 nM agent for 6 h. Cells were then treated with 1 nM EGF for 15 min. Cell lysates were separated by SDS–PAGE, blotted to nitrocellulose, and labeled with rabbit anti-phosphoERK1/2 Y202/Y204 antibody followed by peroxidase-conjugated anti-rabbit antibody and imaged. (**b**) Inhibition of proliferation. hMEC cells with autocrine EGF signaling were cultured in 96-well plates and treated with 20 nM of the indicated agent(s). Additional agent is added after 48 h. Viability is quantified using AlamarBlue and normalized independently for both time points relative to PBSA-treated cells. – or + indicates the absence or presence of 225 antibody. (**c**) EGFR downregulation with Fn3-Fn3 and 225. A431, HeLa and HT29 cells were cultured, serum starved and treated with 20 nM 225 and 20 nM of the indicated Fn3 or Fn3-Fn3 construct for 6–8 h. Surface EGFR was quantified by flow cytometry and is presented on an intensity scale relative to PBSA-treated control with black indicating no downregulation and white indicating complete downregulation. (**d, e**) Inhibition of migration. Cells (TCT in (d), as indicated in (e)) were cultured in 96-well plates to a confluent monolayer. A 'wound' was scratched into each monolayer to create a void of cells. Cells were treated with 20 nM of the indicated agent(s). Migration was analyzed by microscopy. – or + indicates the absence or presence of 225 antibody. Multiple 'wounds' treated with PBSA were completely healed, thus limiting measurable migration. ND indicates no data.

effectively downregulated. Conversely, D-B and D-C heterodimers are able to downregulate transfected EGFR (Fig. 4a). These results indicate a divergence between the mechanisms of downregulation by EGF and Fn3-Fn3 heterodimers. To further explore the mechanism, eight EGFR mutants with point mutations in their intracellular domains were tested for their ability to be downregulated. All eight mutants (T654A, T669A, K721R, Y845F, S1046A/S1047A, Y1068F, Y1148F and Y1173F) exhibit downregulation on par with wild-type EGFR in the presence of D-B and D-C (Fig. 4b). Note in particular that EGFR kinase activity is not required for downregulation, as the K721R mutant was downregulated by D-B and D-C.

The impact of heterodimers on EGFR phosphorylation was analyzed at eight sites: T654, T669, Y845, S1046, Y1068, Y1086, Y1148 and Y1173. Heterobivalent D-C, PBSA or EGF was added to A431 cells for 5, 15, 60 or 240 min and receptor phosphorylation was quantified by in-cell western blot. Receptor agonism by D-C is consistently lower than that by EGF, at near background levels, with the lone exception of T669 at early times (Fig. 4c).

Likewise, standard western blot analysis of cell lysates reveals that heterodimers do not yield significant phosphorylation of ERK1/2 at Y202/Y204 upon 15-min incubation whereas EGF is activating (data not shown). This result is corroborated by global phosphorylation analysis of A431 cells upon addition of heterodimers for 15 or 60 min. Cells were treated with 20 nM agent and phosphorylated tyrosine peptides were analyzed by iTRAQ LC–MS/MS. EGF yields substantially more phosphorylation than heterodimers or a

pair of monovalents (Fig. 4d). Collectively, these data demonstrate that select Fn3-Fn3 heterodimers substantially downregulate EGFR in a manner distinct from EGF and, importantly, without significant receptor activation.

EGFR trafficking material balance

EGFR trafficking can be examined with a model accounting for the four rate processes of synthesis, endocytosis, degradation and recycling (see Supplementary data for further detail). The steady-state surface receptor concentration, S_{ss}, can be solved analytically:

$$S_{ss} = \frac{k_{synthesis}}{k_{endocytosis}}\left(1 + \frac{k_{recycling}}{k_{degradation}}\right) \quad (1)$$

where k terms represent the rate constants of the subscripted processes. Thus, surface receptor can be downregulated via three kinetic mechanisms: decreased synthesis, increased endocytosis or decreased recycling fraction ($k_{recycle}/k_{degradation}$). Reduced synthesis would yield proportional receptor downregulation, but in the absence of measurable EGFR signaling caused by heterodimer treatment, it is difficult to conceive of a feedback mechanism that might reduce EGFR expression. The observed time scale for net internalization (Fig. 3b,c) is significantly slower than reported for first-pass endocytosis of EGFR (Herbst *et al*., 1994; Hoffman and Carlin, 1994), and so accelerated endocytosis is not consistent with the observed downregulation. A five-fold increase in the rate of endocytosis would be required to yield 80% downregulation.

In the limit of fully inhibited recycling, downregulation is bounded by the following limit:

$$\frac{S_{ss,\,no\,recycle}}{S_{ss,\,recycle}} = \frac{1}{1 + k_{recycle}/k_{degradation}} \quad (2)$$

and the kinetics of downregulation is solely driven by endocytosis kinetics, i.e. the half-time for downregulation is equal to the constitutive endocytic half-time. The experimental results are consistent with a reduced recycling fraction (either through enhanced degradation or inhibition of recycling) as 80% downregulation can be achieved with elimination of an original 4:1 recycling:degradation ratio, which is reasonable (French and Lauffenburger, 1996). Various heterodimers may still allow some recycling, resulting in reduced downregulation. From a kinetic standpoint, the 0.4–1.4 h half-time for downregulation is consistent with the constitutive internalization rates for EGFR (Herbst *et al*., 1994; Hoffman and Carlin, 1994). A decreased recycling fraction is the most consistent mechanism of downregulation via heterobivalent Fn3 domain constructs.

Inhibition of signaling, growth, and migration

The ability of monovalent, homobivalent and heterobivalent constructs to inhibit downstream signaling was examined. The downregulating heterodimers A-D, D-B, D-C and D-E inhibit EGF-induced ERK phosphorylation at tyrosines 202 and/or 204 whereas non-downregulating B-B homobivalent has no effect. The monovalent EGF competitor clone D is also antagonistic (Fig. 5a).

The effect of these heterodimers on cellular behavior was examined in terms of proliferation and migration. An autocrine model system was used in which hMEC cells are transfected with a vector for a membrane-bound EGF ligand with an EGF or TGFα cytoplasmic tail (hMEC + ECT or hMEC + TCT; Joslin *et al*., 2007). Treatment with downregulating heterodimers significantly reduced the number of viable cells at 48 and 96 h (Fig. 5b). In addition, combination treatment of 225 antibody and heterodimer further reduces cell viability. The A-D heterodimer in particular downregulates EGFR in the presence of 225 (Fig. 5c). Likewise, treatment with downregulating heterodimer strongly reduces cell migration in the autocrine cells as well as parental hMEC cells, and combination treatment further augments this inhibition (Fig. 5d and e).

Discussion

We report here the engineering of heterodimeric proteins that efficiently downregulate EGFR surface levels without activating the receptor. The wide variation in effects of the combinations of monovalent and homo- and hetero-bivalent constructs strongly suggests the existence of stereospecific constraints on binding-induced downregulation, as opposed to simple gross clustering. As expected, monovalent binding alone does not reduce EGFR levels. Homodimers, aside from weak downregulation by D-D, also are ineffective. In fact, strong reduction in EGFR levels is only observed for selected heterodimers of non-competitive clones. Constructs D-B, D-C, and D-E yield the strongest downregulation whereas A-D, B-D, C-D, and E-D exhibit modest efficacy. Non-competitive heterodimers including clone D, which binds to a novel epitope at the junction of domains III and IV, are generally effective except for D-A. Non-competitive heterodimers including clone A are less consistent. C-A and A-B are weakly effective against all three cell types; A-C and A-E are weakly effective against only two cell types; and B-A and E-A are ineffective. Thus, a combination of non-competitive clones is necessary but not sufficient for strong downregulation. Non-competitive heterobivalent constructs are theoretically topologically able to form receptor clusters because of the ability to bind two heterodimers to a single receptor thereby propagating receptor linkages whereas homobivalents or competitive heterodimers can only form two-receptor complexes. Meanwhile, the reduced efficacy of some non-competitive heterodimers may arise from the inability to simultaneously bind two receptors given the distance and steric constraints of the epitopes targeted and the length of the bivalent linker. pH-dependent binding effects may also play a role.

The heterodimers elicit a response that is qualitatively distinct from that resulting from EGF binding. This is perhaps most clearly demonstrated by the ability of heterodimers to downregulate EGFR overexpressed in HEK cells, which EGF fails to downregulate, perhaps due to a saturation of the endocytic machinery. Also, multiple receptor mutants, including kinase inactive K721R, are downregulated to the same extent as wild-type receptor. Mutation of neither T669 nor S1046, whose phosphorylations are implicated in receptor internalization (Countaway *et al*., 1992; Winograd-Katz and Levitzki, 2006), nor T654, whose phosphorylation either inhibits ubiquitination or accelerates recycling (Bao *et al*., 2000), impacts downregulation. In addition, mutation of Y845, Y1068, Y1148 or Y1173, which are important in the

ERK signaling pathway (Downward *et al*., 1985; Yamauchi *et al*., 1997; Biscardi *et al*., 1999; Wu *et al*., 2002; Amos *et al*., 2005; Morandell *et al*., 2008), has no effect on Fn3-heterodimer-induced downregulation. These results are corroborated by phosphorylation analyses. Seven of the eight key sites studied on EGFR, with the exception of T669, demonstrated significantly lower phosphorylation with heterobivalent D-C compared to EGF stimulation. Conversely, no phosphorylation is observed at T654, S1046 and Y1068. Y845, Y1086, Y1148 and Y1173 exhibit no agonism at multiple time points and weak phosphorylation at 1 h. Moreover, western blot analysis demonstrates ERK phosphorylation upon treatment with EGF but not upon treatment with any of the heterodimers tested. Global phosphoproteomic analysis also exhibits substantially more phosphorylation from EGF than D-B, D-C, or a combination of B and D monomers. Thus, unlike EGF, Fn3-Fn3 constructs achieve receptor downregulation without significant receptor agonism.

A simple mathematical analysis of receptor trafficking indicates that steady-state downregulation is likely to arise from enhanced degradation/recycling ratio. Experimental data suggest that receptor internalization is not increased, as monovalent clone B and downregulating D-B constructs exhibit equivalent intracellular accumulation. Moreover, the kinetics of downregulation ($\tau_{1/2} = 0.4–1.4$ h) are comparable to constitutive receptor internalization kinetics. Thus, although receptor internalization may be increased slightly, it does not appear to be a significant contributor to downregulation. Enhanced degradation could conceivably result from the presence of receptor clusters that either inhibit recycling or drive degradation. In fact, AlexaFluor488-conjugated 225 antibody exhibits reduced recycling in the presence of downregulating heterobivalent A-D as compared to co-treatment with monomer A or non-downregulating C-B (Supplementary data).

This panel of engineered fibronectin domains should provide useful reagents for a variety of applications. The small size of these agents should provide rapid clearance for *in vivo* imaging applications and close proximity of binding site and fluorophore for Förster resonance energy transfer studies. The engineered domains are cysteine-free with primary amines located distal to the presumed binding site with two exceptions: clone H contains a cysteine and lysine in the FG loop and clone D contains adjacent cysteines in the FG loop. Thus, the domains are amenable to thiol and amine chemical conjugation to fluorophores, nanoparticles, drug payloads and chemically modified surfaces for drug delivery, diagnostic and biotechnology applications. The single-domain architecture readily enables protein fusion such as the heterodimers discussed herein and immunotoxins (Pirie *et al*., 2011). The picomolar to low nanomolar binding of these domains is sufficient for most applications. The breadth of epitopes targeted is useful for biophysical studies and dual binding such as for receptor clustering or sandwich immunoassays.

Downregulation decreases the amount of receptor available for ligand binding, receptor homo- and hetero-dimerization and constitutive activation, thereby decreasing the opportunity for receptor signaling. Downregulation is sufficient to inhibit ligand-induced phosphorylation of ERK, a downstream signaling molecule on a pathway that leads to proliferation and migration. The heterodimers reported here inhibit proliferation and migration of a cell line with autocrine signaling, and this inhibitory activity can be augmented by combination treatment with antibody 225, which can provide additional crosslinking and ligand competition. The ability to significantly downregulate EGFR with minimal agonism, while decreasing cell proliferation and cell migration, highlight the promise of these engineered heterodimers as components of novel potential cancer therapeutics.

Supplementary data

Supplementary data are available at *PEDS* online.

Acknowledgements

The work was supported by the National Institutes of Health grant CA96504 (K.D.W), grant CA118705 (F.M.W.), and National Science Foundation Graduate Fellowship (B.J.H.). Steve Sazinsky produced the EGFR ectodomain. Jamie Spangler performed quantification of surface EGFR levels.

Author contributions

B.J.H. designed research, performed experiments, and wrote and edited the paper. J.R.N. performed proteomic mass spectrometry experiments and edited the paper. F.M.W. edited the paper. K.D.W. designed research and wrote and edited the paper.

References

Ackerman,M., Levary,D., Tobon,G., *et al*. (2009) *Biotechnol Prog*, **25**, 774–783.
Amos,S., Martin,P.M., Polar,G.A., *et al*. (2005) *J Biol Chem*, **280**, 7729–7738.
Bao,J., Alroy,I., Waterman,H., *et al*. (2000) *J Biol Chem*, **275**, 26178–26186.
Ben-Kasus,T., Schechter,B., Lavi,S., *et al*. (2009) *Proc Natl Acad Sci USA*, **106**, 3294–3299.
Biscardi,J.S., Maa,M.C., Tice,D.A., *et al*. (1999) *J Biol Chem*, **274**, 8335–8343.
Bonner,J.A., Harari,P.M., Giralt,J., *et al*. (2006) *N Engl J Med*, **354**, 567–578.
Burgess,A., Cho,H.S., Eigenbrot,C., *et al*. (2003) *Mol Cell*, **12**, 541–552.
Chao,G., Cochran,J.R. and Wittrup,K. (2004) *J Mol Biol*, **342**, 539–550.
Cochran,J.R., Kim,Y., Olsen,M.J., *et al*. (2004) *J Immunol Methods*, **287**, 147–158.
Countaway,J.L., Nairn,A.C. and Davis,R.J. (1992) *J Biol Chem*, **267**, 1129–1140.
Cunningham,D., Humblet,Y., Siena,S., *et al*. (2004) *N Engl J Med*, **351**, 337–345.
Downward,J., Waterfield,M.D. and Parker,P.J. (1985) *J Biol Chem*, **260**, 14538–14546.
Ferguson,K.M., Berger,M.B., Mendrola,J.M., *et al*. (2003) *Mol Cell*, **2003**, 507–517.
French,A.R. and Lauffenburger,D.A. (1996) Biotechnol Bioeng, **51**, 281–297.
Friedman,L.M., Rinon,A., Schechter,B., *et al*. (2005) *Proc Natl Acad Sci USA*, **102**, 1915–1920.
Hackel,B.J., Kapila,A. and Wittrup,K.D. (2008) *J Mol Biol*, **381**, 1238–1252.
Hackel,B.J., Ackerman,M., Howland,S.W., *et al*. (2010) *J Mol Biol*, **401**, 84–96.
Herbst,J.J., Opresko,L.K., Walsh,B.J., *et al*. (1994) *J Biol Chem*, **269**, 12865–12873.
Hoffman,P. and Carlin,C. (1994) *Mol Cell Biol*, **14**, 3695–3706.
Joslin,E.J., Opresko,L.K., Wells,A., *et al*. (2007) *J Cell Sci*, **120**(Pt 20), 3688–3699.
Kim,Y., Bhandari,R., Cochran,J., *et al*. (2006) *Proteins*, **62**, 1026–1035.
Koide,A. and Koide,S. (2007) *Methods Mol Biol*, **352**, 95–109.
Lee,J.C., Vivanco,I., Beroukhim,R., *et al*. (2006) *PLoS Med*, **3**, e485.
Li,S., *et al*. (2005) *Cancer Cell*, **7**, 301–311.

Messersmith,W. and Hidalgo,M. (2007) *Clin Cancer Res*, **13**, 4664–4666.
Morandell,S., Stasyk,T., Skvortsov,S., *et al*. (2008) *Proteomics*, **8**, 4383–4401.
Nicholson,R.I., Gee,J.M. and Harper,M.E. (2001) *Eur J Cancer*, **37**(Suppl 4), S9–S15.
Ogiso,H., Ishitani,R., Nureki,O., *et al*. (2002) *Cell*, **110**, 775–787.
Pedersen,M.W., Meltorn,M., Damstrup,L., *et al*. (2001) *Ann Oncol*, **12**, 745–760.
Perera,R., Narita,Y., Furnari,F.B., *et al*. (2005) *Clin Cancer Res*, **11**, 6390–6399.
Pirie,C.M., Hackel,B.J., Rosenblum,M.G., *et al*. (2011) *J Biol Chem*, **286**, 4165–4172.
Sharma,S.V., Bell,D.W., Settleman,J., *et al*. (2007) *Nat Rev Cancer*, **7**, 169–181.
Spangler,J.B., Neil,J.R., Abramovitch,S., *et al*. (2010) *Proc Natl Acad Sci USA*, **107**, 13252–13257.
Tateishi,M., Ishida,T., Mitsudomi,T., *et al*. (1990) *Cancer Res*, **50**, 7077–7080.
Winograd-Katz,S.E. and Levitzki,A. (2006) *Oncogene*, **25**, 7381–7390.
Wu,W., Graves,L.M., Gill,G.N., *et al*. (2002) *J Biol Chem*, **277**, 24252–24257.
Yamauchi,T., Ueki,K., Tobe,K., *et al*. (1997) *Nature*, **390**, 91–96.
Yarden,Y. and Sliwkowski,M.X. (2001) *Nat Rev Mol Cell Biol*, **2**, 127–137.